

Enhanced thermopower under a time-dependent gate voltage

 Adeline Crépieux,¹ Fedor Šimkovic,¹ Benjamin Cambon,¹ and Fabienne Michelini²
¹*Centre de Physique Théorique, Aix-Marseille Université, 163 avenue de Luminy, F-13288 Marseille, France*
²*Institut Matériaux Microélectronique Nanosciences de Provence, Aix-Marseille Université, Avenue Escadrille Normandie Niemen, F-13397 Marseille, France*

(Received 22 February 2011; published 25 April 2011)

We derive formal expressions of time-dependent energy and heat currents through a nanoscopic device using the Keldysh nonequilibrium Green function technique. Numerical results are reported for a metal-dot-metal junction where the dot level energy is abruptly changed by a step-shaped voltage pulse. Analytical linear responses are obtained for the time-dependent thermoelectric coefficients. We show that in the transient regime the Seebeck coefficient can be enhanced by an amount (as much as 40%) controlled by both the dot energy and the height of the voltage step.

 DOI: [10.1103/PhysRevB.83.153417](https://doi.org/10.1103/PhysRevB.83.153417)

PACS number(s): 44.05.+e, 72.15.Jf, 73.63.Kv

Since their discoveries in 1821 by Seebeck¹ and in 1834 by Peltier,² thermoelectric effects have been exploited for many applications, such as heat voltage converters, thermocouples, or refrigerators. The Seebeck coefficient, or thermopower S , measures the voltage induced by a temperature gradient through an open circuit, whereas the Peltier coefficient Π measures the heat flow induced by an applied current for no temperature gradient. In the linear response regime, the Onsager relation gives $\Pi = -ST$, where T is the average temperature of the sample.

Recent achievements in the field of nanoscale systems have invigorated research activities in this area and renewed the quest for enhanced thermopower (see Ref. 3 for a recent review). Stationary Seebeck coefficients have been measured in different nanoscale systems: quantum dots,⁴ atomic-size contacts,⁵ spin valves,⁶ nanowires,⁷ and carbon nanotubes.⁸ The Landauer-Büttiker formalism used for the electrical conductance was extended to model thermal transport in microstructures with many terminals,^{9,10} including inelastic effects.¹¹ The validity of conventional thermodynamic linear equations was deeply questioned in mesoscopic systems: the Onsager relations between heat and charge transport coefficients,^{9,12} the Wiedemann-Franz law, which links electrical and thermal conductances,¹³ and the Fourier law.¹⁴ Time-dependent electric transport also benefits from active research works. Single-electron time-control has been demonstrated experimentally^{15,16} with a fair agreement with earlier theoretical developments.^{17,18} More recently, deeper issues, such as memory effects¹⁹ or interplay between multiple time modulations,²⁰ have been addressed theoretically. In addition, calculation of time-dependent heat current in a linear phonon chain has recently been achieved,²¹ and energy balance in nanoscale junctions has been considered.²² However, thermopower dynamics lacks both experimental and theoretical investigations.

This Brief Report gives insight into time-dependent nonequilibrium thermoelectric transport. As a major result, illustrated in Fig. 1, we show that the thermopower can be strongly enhanced during the transient regime in a metal-dot-metal device (schematically presented in Fig. 2). The time evolution of the thermopower exhibits promising features. Indeed, it can be significantly modified and controlled by

changing the dot energy from $\tilde{\epsilon}_0$ to $\tilde{\epsilon}_0 + \tilde{\gamma}_0$ at time $t_0 = 0$: starting from the stationary value at $t < t_0$, it increases during a finite time interval, and then it converges toward its new stationary value at $t \rightarrow \infty$.

The time-dependent heat current through the left (L) or the right (R) reservoir in equilibrium reads

$$\langle I_{L,R}^h(t) \rangle = \langle I_{L,R}^E(t) \rangle - \frac{\mu_{L,R}(t)}{e} \langle I_{L,R}^e(t) \rangle, \quad (1)$$

where $\langle I_{L,R}^E(t) \rangle$ is the energy current, $\langle I_{L,R}^e(t) \rangle$ is the electric current, and $\mu_{L,R}$ is the chemical potential. The time-dependent Seebeck coefficient can be obtained from the ratio between the voltage gradient ΔV and the temperature gradient ΔT between the two reservoirs, when both left and right time-dependent electric currents cancel:

$$S(t) = - \frac{\Delta V}{\Delta T} \Big|_{\langle I_L^e(t) \rangle = \langle I_R^e(t) \rangle = 0}, \quad (2)$$

whereas the time-dependent Peltier coefficient is defined as

$$\Pi(t) = \frac{\langle I_L^h(t) \rangle - \langle I_R^h(t) \rangle}{\langle I_L^e(t) \rangle - \langle I_R^e(t) \rangle} \Big|_{\Delta T=0}. \quad (3)$$

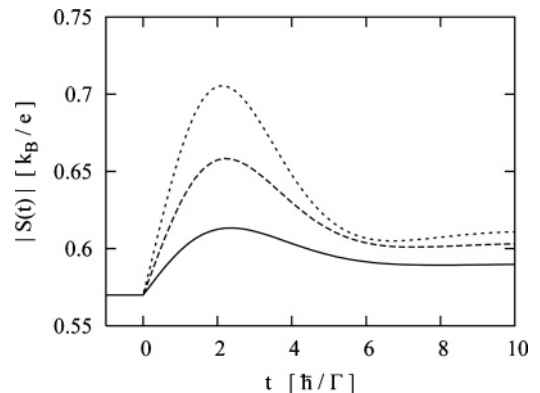


FIG. 1. Increase of the Seebeck coefficient in the transient regime of a metal-dot-metal junction: $\tilde{\epsilon}_0 = 0.5$ with $\tilde{\gamma}_0 = 0.05$ (solid line), $\tilde{\gamma}_0 = 0.1$ (dashed line), and $\tilde{\gamma}_0 = 0.15$ (dotted line). We take symmetric barriers $\Gamma_R = \Gamma_L$, $t_0 = 0$, $\epsilon_F = 0$, and $k_B T = 0.1$. The unit of energy is Γ .

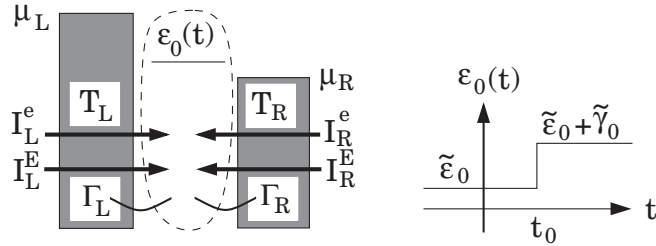


FIG. 2. Left panel: Schematic representation of a metal-dot-metal junction with current directions for each lead. Right panel: Time dependence of the dot energy level. We define the chemical potentials and the temperatures of the left and right leads as $\mu_{L,R} = \varepsilon_F \pm e\Delta V/2$ and $T_{L,R} = T \pm \Delta T/2$. The Fermi energy is ε_F and $T = (T_R + T_L)/2$ is the average temperature.

The general system we consider consists of N energy levels in an interacting central region connected to noninteracting left and right leads. The total Hamiltonian reads $H = H_L + H_R + H_c + H_T$ with

$$H_{L,R} = \sum_{k \in L,R} \varepsilon_k(t) c_k^\dagger c_k, \quad (4)$$

$$H_c = \sum_n \varepsilon_n(t) d_n^\dagger d_n + H_{\text{int}}, \quad (5)$$

$$H_T = \sum_{p=L,R} \sum_{k \in p,n} V_{kn}(t) c_k^\dagger d_n + \text{H.c.}, \quad (6)$$

where c_k^\dagger (d_n^\dagger) and c_k (d_n) are the creation and annihilation operators for the leads (dot), and H_{int} is the interacting part of H_c (Coulomb interactions, phonon coupling, etc.). The energy band ε_k of the reservoirs can be time dependent through a bias change (source-drain voltage). The energy levels of the central region, ε_n , can be time dependent through a modulation of the gate voltage. For the sake of generality, the hopping amplitudes, V_{kn} , are also allowed to be time dependent. Extension to multiterminal systems with additional degrees of freedom (e.g., spin) is straightforward. In this calculation we only consider the electron contribution to the energy current.

The energy current operator is related to the time derivative of the Hamiltonian describing the leads²³ by $I_{L,R}^E = -\dot{H}_{L,R}$. After calculating the commutators $[H_{L,R}, H]$, we end up with ($\hbar = 1$)

$$I_{L,R}^E(t) = i \sum_{k \in L,R,n} \varepsilon_k(t) V_{kn}(t) c_k^\dagger d_n + \text{H.c.} - \sum_{k \in L,R} \dot{\varepsilon}_k(t) c_k^\dagger c_k. \quad (7)$$

Thus, the average energy current reads

$$\langle I_{L,R}^E(t) \rangle = 2\text{Re} \left\{ \sum_{k \in L,R,n} \varepsilon_k(t) V_{kn}(t) G_{nk}^<(t,t) \right\} - \text{Im} \left\{ \sum_{k \in L,R} \dot{\varepsilon}_k(t) G_{kk}^<(t,t) \right\}, \quad (8)$$

where $G_{kk}^<(t,t') = i \langle c_k^\dagger(t') c_k(t) \rangle$ is the lead Green function. We have introduced the mixed Green function $G_{nk}^<(t,t') = i \langle c_k^\dagger(t') d_n(t) \rangle$, which obeys the Dyson equation

$$G_{nk}^<(t,t') = \sum_{n'} \int_{-\infty}^{\infty} dt_1 V_{kn'}^*(t_1) [G_{nn'}^r(t,t_1) g_k^<(t_1,t') + G_{nn'}^<(t,t_1) g_k^a(t_1,t')]. \quad (9)$$

$G_{nn'}^<(t,t') = i \langle d_n^\dagger(t') d_n(t) \rangle$ is the dot Green function. $g_k^<(t,t') = i f(\varepsilon_k) e^{-i \int_{t'}^t dt_1 \varepsilon_k(t_1)}$ and $g_k^a(t,t') = i \Theta(t' - t) e^{-i \int_t^{t'} dt_1 \varepsilon_k(t_1)}$ are the Green functions of the isolated leads. The expression of the energy current becomes

$$\langle I_{L,R}^E(t) \rangle = 2\text{Re} \left\{ \text{Tr} \left\{ \int_{-\infty}^{\infty} dt_1 [G_d^r(t,t_1) \Xi_{L,R}^<(t_1,t) + G_d^<(t,t_1) \Xi_{L,R}^a(t_1,t)] \right\} - \text{Im} \left\{ \sum_{k \in L,R} \dot{\varepsilon}_k(t) G_{kk}^<(t,t) \right\} \right\}, \quad (10)$$

where we have defined the self-energy associated with energy transfer as $\Xi_{L,R}^{a,<}(t,t') = \sum_{k \in L,R} \mathbf{V}_k^*(t) g_k^{a,<}(t,t') \varepsilon_k(t') \mathbf{V}_k(t')$. In these expressions, \mathbf{V}_k is a vector whereas $G_d^{a,<}$ and $\Xi_{L,R}^{a,<}$ are matrices. The last term in Eq. (10) is a pure reservoir contribution to the energy current.

We now consider a noninteracting metal-dot-metal junction with a single dot level ε_0 connected to reservoirs with constant energy bands. This model is suitable for experiments in which the Coulomb interaction is weak in the dot with strong coupling to reservoirs.^{15,24} In that case, the energy current takes the form

$$\langle I_{L,R}^E(t) \rangle = 2\text{Re} \left\{ \int_{-\infty}^{\infty} dt_1 \int_{-\infty}^{\infty} \frac{d\varepsilon}{2\pi} i \varepsilon e^{i\varepsilon(t-t_1)} \Gamma_{L,R}(\varepsilon, t_1, t) \times [G_d^r(t,t_1) f_{L,R}(\varepsilon) + G_d^<(t,t_1) \Theta(t-t_1)] \right\}, \quad (11)$$

where Θ is the Heaviside function, $f_{L,R}$ is the Fermi-Dirac distribution function, $\rho_{L,R}$ is the density of states, and $\Gamma_{L,R}(\varepsilon_k, t, t') = 2\pi \rho_{L,R}(\varepsilon_k) V_k^*(t) V_k(t')$ measures the strength of the coupling between the dot and each lead.

We investigate the time-dependent thermoelectric response to a unique change $\varepsilon_0(t) = \tilde{\varepsilon}_0 + \gamma_0(t)$ with $\gamma_0(t) = \tilde{\gamma}_0 \Theta(t - t_0)$. This models a dot energy switching from $\tilde{\varepsilon}_0$ to $\tilde{\varepsilon}_0 + \tilde{\gamma}_0$ by applying a gate voltage at t_0 (see Fig. 2). The time-dependent heat current defined by Eq. (1) for $p = L, R$ is now expressed in terms of the spectral function $A(\varepsilon, t)$ as

$$\langle I_p^h(t) \rangle = -\frac{1}{h} \Gamma_p \left[2 \int_{-\infty}^{\infty} (\varepsilon - \mu_p) f_p(\varepsilon) \text{Im}\{A(\varepsilon, t)\} d\varepsilon + \sum_{p'=L,R} \Gamma_{p'} \int_{-\infty}^{\infty} (\varepsilon - \mu_{p'}) f_{p'}(\varepsilon) |A(\varepsilon, t)|^2 d\varepsilon \right], \quad (12)$$

with¹⁷

$$A(\varepsilon, t) = \frac{\varepsilon - \tilde{\varepsilon}_0 + i\Gamma/2 - \tilde{\gamma}_0 e^{i(t-t_0)(\varepsilon - \tilde{\varepsilon}_0 - \tilde{\gamma}_0 + i\Gamma/2)}}{(\varepsilon - \tilde{\varepsilon}_0 + i\Gamma/2)(\varepsilon - \tilde{\varepsilon}_0 - \tilde{\gamma}_0 + i\Gamma/2)}, \quad (13)$$

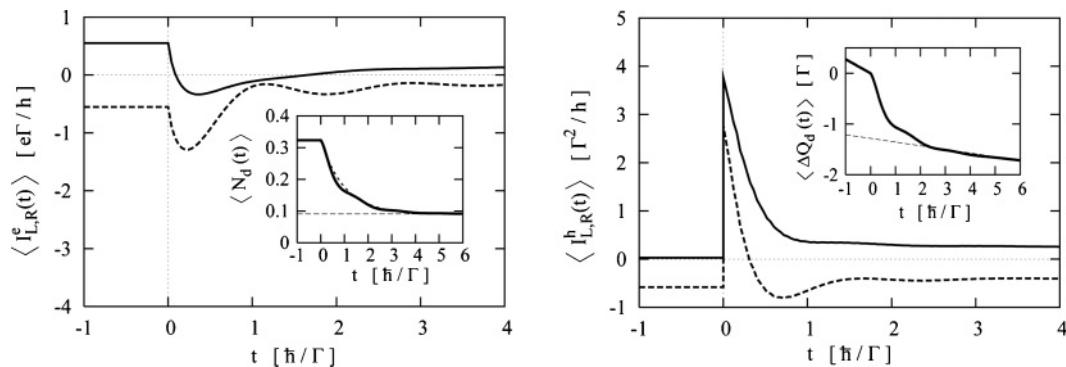


FIG. 3. Electric current (left panel) and heat current (right panel) through the left lead (solid lines) and the right lead (dashed lines) as a function of time t , for $\Gamma_R = \Gamma_L$, $t_0 = 0$, $\tilde{\varepsilon}_0 = 0.5$, $\tilde{\gamma}_0 = 2.5$, $k_B T_L = 1$, $k_B T_R = 0$, and $\mu_{L,R} = \pm 0.5$. The insets show the dot occupation (left inset) and the dot heat (right inset). Dashed lines indicate the stationary limits at $t \rightarrow \infty$. The unit of energy is Γ .

and $\Gamma = \Gamma_L + \Gamma_R$, for which we assume that Γ_p does not depend on energy (wide-band limit) and simply reduces to $\Gamma_p = 2\pi\rho_p|V_p|^2$.

The integration over energy in Eq. (12) has been performed numerically. In Fig. 3 the time evolution of electric and heat currents when the dot energy is modified abruptly at $t_0 = 0$ is plotted. Starting from constant values at $t < 0$, the left and right currents converge toward constant values at $t \rightarrow \infty$. Between these two limits, currents show strong time-dependent variations. Currents through the zero temperature, $T_R = 0$, in the right lead (see dashed lines in Fig. 3) exhibit time oscillations whose period is related to $\tilde{\varepsilon}_0$ and $\tilde{\gamma}_0$, as Eq. (13) explicitly indicates. These oscillations of the electric current have been measured through a Ge dot.¹⁶ Regarding the heat current, experimental results are still needed. In the left lead (see solid lines in Fig. 3) these oscillations disappear due to thermal effects given by $T_L \neq 0$.

Using particle number conservation, the average dot occupation number is calculated from electric currents as $\langle N_d(t) \rangle = e^{-1} \int \langle I_{\text{dis}}^e(t) \rangle dt$, where $I_{\text{dis}}^e(t) = I_L^e(t) + I_R^e(t)$ is the displacement current.¹⁶ In the left inset of Fig. 3, $\langle N_d(t) \rangle$ globally follows an exponential decrease $\langle N_d(\infty) \rangle (1 - e^{-t/\tau_r}) + \langle N_d(0) \rangle e^{-t/\tau_r}$ (see dotted line) characterized by the relaxation time $\tau_r = \hbar/\Gamma$; the weaker is the coupling between the dot and the leads the longer is the relaxation time. The time evolution of $\langle N_d(t) \rangle$ shows oscillations around this decrease that have been already observed in experiments.¹⁶

Equation (1) comes from thermodynamic relations in the leads at equilibrium: $dH_{L,R} = dQ_{L,R} + \mu_{L,R}dN_{L,R}$, where $N_{L,R}$ is the lead occupation number and $Q_{L,R}$ is the lead heat. Similarly, for the dot out of equilibrium we write $dH_c = dQ_d - \mu_L dN_L - \mu_R dN_R$; the energy change in the dot reflects a balance between heat variation and charges leaving the dot times their energies. Thus, we define and numerically calculate an average heat in the dot as $\langle Q_d(t) \rangle = \int \langle I_d^h(t) \rangle dt$, where $I_d^h(t) = I_L^h(t) + I_R^h(t) - \dot{H}_T(t)$. This definition perfectly agrees with energy conservation including a contribution from tunneling. In the right inset of Fig. 3, the time evolution of $\langle \Delta Q_d(t) \rangle = \langle Q_d(t) \rangle - \langle Q_d(0) \rangle$ shows a behavior similar to the dot occupation number (left inset of Fig. 3). However, dramatic differences occur in the stationary regimes, for which $\langle N_d(t) \rangle$ is always constant, e.g., the dot

heat increases linearly with time, which is known as the Joule effect.

In the linear response limit, the time-dependent Seebeck coefficient, defined by Eq. (2), can be obtained from the approximate Fermi-Dirac distribution function⁹ $f_{L,R}(\varepsilon) \approx f_0(\varepsilon) + f'_0(\varepsilon)[\mu_{L,R} - (\varepsilon - \varepsilon_F)T_{L,R}/T]$, where f_0 is the Fermi-Dirac distribution function for the leads when $\mu_L = \mu_R$. Taking the left and right electric currents equal to zero, we obtain the linear response for $S(t)$ in the case of strong coupling to reservoir and small energy variation:

$$S(t) = -\frac{\int_{-\infty}^{\infty} d\varepsilon f'_0(\varepsilon)(\varepsilon - \varepsilon_F)\mathcal{T}(\varepsilon, t)}{eT \int_{-\infty}^{\infty} d\varepsilon f'_0(\varepsilon)\mathcal{T}(\varepsilon, t)}, \quad (14)$$

where $\mathcal{T}(\varepsilon, t) = -2\Gamma_L\Gamma_R\text{Im}\{A(\varepsilon, t)\}/\Gamma$ is the time-dependent transmission coefficient. This result is a generalization of the Seebeck coefficient expression obtained in the stationary case^{3,9} including the time dependence of the transmission coefficient. For the steady-state situation we have $\langle I_L^e \rangle = -\langle I_R^e \rangle$ [constant $\langle N_d(t) \rangle$], as can be seen in the left panel of Fig. 3. But in the time-dependent case, $\langle I_L^e(t) \rangle = 0$ does not imply $\langle I_R^e(t) \rangle = 0$ because of the displacement current. Since the Seebeck coefficient is measured in an open circuit, we must find the adequate ΔV and ΔT that simultaneously

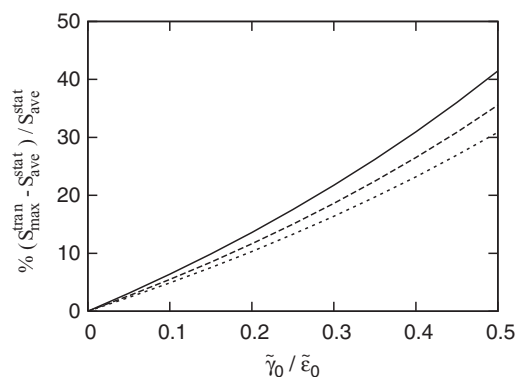


FIG. 4. Percentage of increase of the Seebeck coefficient in the transient regime $S_{\text{max}}^{\text{tran}}$ as a function of $\tilde{\gamma}_0/\tilde{\varepsilon}_0$ for $k_B T = 0.05$ (solid line), $k_B T = 0.15$ (dashed line), and $k_B T = 0.5$ (dotted line). We take $\Gamma_R = \Gamma_L$ and $\varepsilon_F = 0$. The unit of energy is Γ .

cancel both currents. It is important to emphasize that Eq. (14) is only valid under the following assumptions: (i) linear response (small ΔV and ΔT in comparison to $\tilde{\varepsilon}_0$ and T), (ii) high transmission through the barriers (large Γ_L and Γ_R in comparison to other energies), and (iii) small gate voltage time variation $\tilde{\gamma}_0$ in comparison to $\tilde{\varepsilon}_0$. Indeed, these assumptions allow us to approximate $|A(\varepsilon, t)|^2 \approx -2\text{Im}[A(\varepsilon, t)]/\Gamma$, and, hence, to cancel both $\langle I_L^c(t) \rangle$ and $\langle I_R^e(t) \rangle$ at any time.

Following the same assumptions, a similar expression can be obtained for the time-dependent Peltier coefficient defined by Eq. (3),

$$\Pi(t) = \frac{\int_{-\infty}^{\infty} d\varepsilon (\varepsilon - \varepsilon_F) [f_L(\varepsilon) - f_R(\varepsilon)] \mathcal{T}(\varepsilon, t)}{e \int_{-\infty}^{\infty} d\varepsilon [f_L(\varepsilon) - f_R(\varepsilon)] \mathcal{T}(\varepsilon, t)} \Big|_{\Delta T=0}. \quad (15)$$

In the linear response regime, Eqs. (14) and (15) verify the Onsager relation $\Pi(t) = -TS(t)$ at any time.

Figure 1 is obtained using Eq. (14) of the linear response. It shows an increase of the thermopower after a step-shaped gate-voltage pulse was applied. The reason for the increase is that in the transient regime the system is much more sensitive to temperature or electrostatic variations. Furthermore, we measure the thermoelectric benefit of the transient regime by calculating the percentage $(S_{\max}^{\text{tran}} - S_{\text{ave}}^{\text{stat}})/S_{\text{ave}}^{\text{stat}}$, where S_{\max}^{tran} is the maximum value of S and $S_{\text{ave}}^{\text{stat}} = [S(t < t_0) + S(t \rightarrow \infty)]/2$. In Fig. 4

we have plotted the percentage of thermopower increase as a function of $\tilde{\gamma}_0/\tilde{\varepsilon}_0$. This ratio plays an important role since it does control the thermopower increase. In such a junction, the transient thermopower can be tuned by both $\tilde{\varepsilon}_0$ and $\tilde{\gamma}_0$, which depend on the dot structural properties and on the applied gate voltage (see Fig. 2). The higher the ratio the higher is the thermopower increase. Here, an increase up to 40% is obtained at small temperature.

We have proposed a first approach to heat dynamics in nanoscale junctions. General formulas for the time-dependent heat and energy currents flowing through an interacting resonant-tunneling system have been obtained. We show that an enhanced thermopower can be generated during the transient regime in a metal-dot-metal junction and that its maximum value can be tuned by both the dot energy and the gate voltage. With such numerical investigations, it will be possible to go beyond the linear response for the Seebeck and Peltier coefficients, and further determine nonlinear thermodynamic laws. Moreover, we shall consider interacting systems in order to analyze the phonon-bath contribution²¹ and the impact of electron-phonon interaction,¹¹ and to study the influence of charging effects.²⁵

A.C. thanks I. Safi for discussion and E. Bernardo for her help in bibliographic searches.

¹T. J. Seebeck, Abh. K. Akad. Wiss. 289 (1820); T. J. Seebeck, *ibid.* 265 (1823).

²J. C. A. Peltier, Ann. Phys. Chim. **56**, 371 (1834).

³Y. Dubi and M. Di Ventra, *Rev. Mod. Phys.* **83**, 131 (2011).

⁴R. Scheibner, H. Buhmann, D. Reuter, M. N. Kiselev, and L. W. Molenkamp, *Phys. Rev. Lett.* **95**, 176602 (2005).

⁵B. Ludoph and J. M. van Ruitenbeek, *Phys. Rev. B* **59**, 12290 (1999).

⁶F. L. Bakker, A. Slachter, J.-P. Adam, and B. J. van Wees, *Phys. Rev. Lett.* **105**, 136601 (2010).

⁷A. I. Hochbaum, R. Chen, R. D. Delgado, W. Liang, E. C. Garnett, M. Najarian, A. Majumdar, and P. Yang, *Nature (London)* **451**, 163 (2008); A. I. Boukai, Y. Bunimovich, J. Tahir-Kheli, J.-K. Yu, W. A. Goddard, and J. R. Heath, *ibid.* **451**, 168 (2008).

⁸G. U. Sumanasekera, B. K. Pradhan, H. E. Romero, K. W. Adu, and P. C. Eklund, *Phys. Rev. Lett.* **89**, 166801 (2002); J. P. Small, K. M. Perez, and P. Kim, *ibid.* **91**, 256801 (2003).

⁹P. N. Butcher, *J. Phys. Condens. Matter* **2**, 4869 (1990).

¹⁰U. Sivan and Y. Imry, *Phys. Rev. B* **33**, 551 (1986).

¹¹K. A. Matveev and A. V. Andreev, *Phys. Rev. B* **66**, 045301 (2002); O. Entin-Wohlman, Y. Imry, and A. Aharony, *ibid.* **82**, 115314 (2010); M. Galperin, A. Nitzan, and M. A. Ratner, *ibid.* **75**, 155312 (2007); *Mol. Phys.* **106**, 397 (2008).

¹²E. Iyoda, Y. Utsumi, and T. Kato, *J. Phys. Soc. Jpn.* **79**, 045003 (2010).

¹³M. G. Vavilov and A. D. Stone, *Phys. Rev. B* **72**, 205107 (2005).

¹⁴Y. Dubi and M. Di Ventra, *Nano Lett.* **9**, 97 (2009).

¹⁵G. Fève, A. Mahé, J.-M. Berroir, T. Kontos, B. Plaçais, D. C. Glattli, A. Cavanna, B. Etienne, and Y. Jin, *Science* **316**, 1169 (2007); *Physica E* **40**, 954 (2008).

¹⁶W.-T. Lai, D. M. T. Kuo, and P.-W. Li, *Physica E* **41**, 886 (2009).

¹⁷A.-P. Jauho, N. S. Wingreen, and Y. Meir, *Phys. Rev. B* **50**, 5528 (1994).

¹⁸H. M. Pastawski, *Phys. Rev. B* **46**, 4053 (1992).

¹⁹E. Perfetto, G. Stefanucci, M. Cini, *Phys. Rev. Lett.* **105**, 156802 (2010).

²⁰F. Foieri and L. Arrachea, *Phys. Rev. B* **82**, 125434 (2010).

²¹E. C. Cuansing and J.-S. Wang, *Phys. Rev. B* **81**, 052302 (2010); *Phys. Rev. E* **82**, 021116 (2010).

²²L. Arrachea, M. Moskalets, and L. Martin-Moreno, *Phys. Rev. B* **75**, 245420 (2007).

²³J.-S. Wang, J. Wang, and N. Zeng, *Phys. Rev. B* **74**, 033408 (2006).

²⁴J. Gabelli, G. Fève, J.-M. Berroir, B. Plaçais, A. Cavanna, B. Etienne, Y. Jin, and D. C. Glattli, *Science* **313**, 499 (2006).

²⁵J. Splettstoesser, M. Governale, J. König, and M. Büttiker, *Phys. Rev. B* **81**, 165318 (2010).